

MICROSTRUCTURE AND PROPERTIES OF THIN FILMS OF ZIRCONIUM PRODUCED BY HIGH-FREQUENCY LASER DEPOSITION

N. A. Bosak,^{a,*} A. N. Chumakov,^a L. V. Baran,^b
V. V. Malyutina-Bronskaya,^c M. Ivkovich,^d
N. Sakan,^d and A. A. Ivanov^a

UDC 621.373.826:533.9+537.9

Nanostructured thin films on a silicon substrate were obtained by high-frequency periodic pulse $f \sim 6\text{--}10\text{ kHz}$ action of laser radiation with wavelength $\lambda = 1.064\text{ }\mu\text{m}$ and power density $q = 120\text{ MW/cm}^2$ on zirconium in a vacuum chamber at pressure $p = 2.2\text{ Pa}$. The morphology of the thin films of zirconium was studied by atomic-force microscopy. The transmission spectra of the zirconium films in the visible and near and mid IR regions were obtained. The electrophysical characteristics of the Zr/Si structures were analyzed.

Keywords: high-frequency laser action, thin film structure, transmission and reflection spectra, electrophysical characteristics.

Introduction. Thin films of various materials are widely used in semiconductor electronics, including microelectronics. On account of a series of physicochemical characteristics they are used as buffer coatings resistant to high plasma temperatures, corrosive environments, slow neutrons, solid-state electrolyte materials, etc. [1]. Most promising for the production of protective coatings are titanium and zirconium oxides. In particular, thin films of $\text{Pb}(\text{Zr}, \text{Ti})\text{O}_3$ in silicon, produced by laser deposition under vacuum, are being investigated as ferroelectrics [2].

Zirconium is a metal with a high melting point ($T = 1855^\circ\text{C}$) that has a low neutron capture section, ideal biocompatibility with the tissues of living organisms, and high corrosion resistance over a wide range of temperatures as a result of the fact that a compact protective oxide film of ZrO_2 is formed on the surface during interaction with oxygen. On account of these unique properties Zr is widely used as a structural material for nuclear reactors and for the creation of surgical instruments, implants, and prostheses and also as protective coatings [3–6]. The deposition of Zr on the films of indium tin oxide ITO ($\text{In}_2\text{O}_3)_{0.9}-(\text{SnO}_2)_{0.1}$ used in solar cells increases the work function of the latter and improves the characteristics of solar cells with $a\text{-Si:H}/c\text{-Si}$ heterojunction [7]. In [8] it was established that films with improved optical properties are deposited when ITO and Zr are deposited together.

On account of the above-mentioned properties Schottky diodes are preferred to $p\text{-}n$ diodes for such applications as digital switching, AC/DC converters, radar systems, signal mixing, metal oxide field effect transistors (MOSFET), and infrared (IR) detectors [9].

The physicochemical properties of the Zr films are determined largely by structural features, including the surface morphology, that are mainly determined by the method by which the film is deposited. The presence of localized interface states has a substantial effect on the properties of structures of the Schottky diode type. The barrier height of the structure is also affected by the state of the interface. Thus, deposition of a metal with high work function on a n -semiconductor or of a metal with a low work function to a p -semiconductor does not always give a high barrier height [10]. Zirconium has a work function of 4.05 eV and therefore has high potential for Si [9].

*To whom correspondence should be addressed.

^aInstitute of Physics, National Academy of Sciences of Belarus, Minsk, Belarus; email: n.bosak@ifanbel.bas-net.by;
^bBelarus State University, Minsk, Belarus; email: baran@bsu.by; ^cGNPO "Optics, Optoelectronics, and Laser Technology," National Academy of Sciences, Minsk, Belarus; email: malyutina@oelt.basnet.by; ^dInstitute of Physics, Belgrade, Serbia; email: nsakan@ipb.ac.rs. Translated from *Zhurnal Prikladnoi Spektroskopii*, Vol. 90, No. 6, pp. 877–881, November–December, 2023. Original article submitted July 20, 2023.

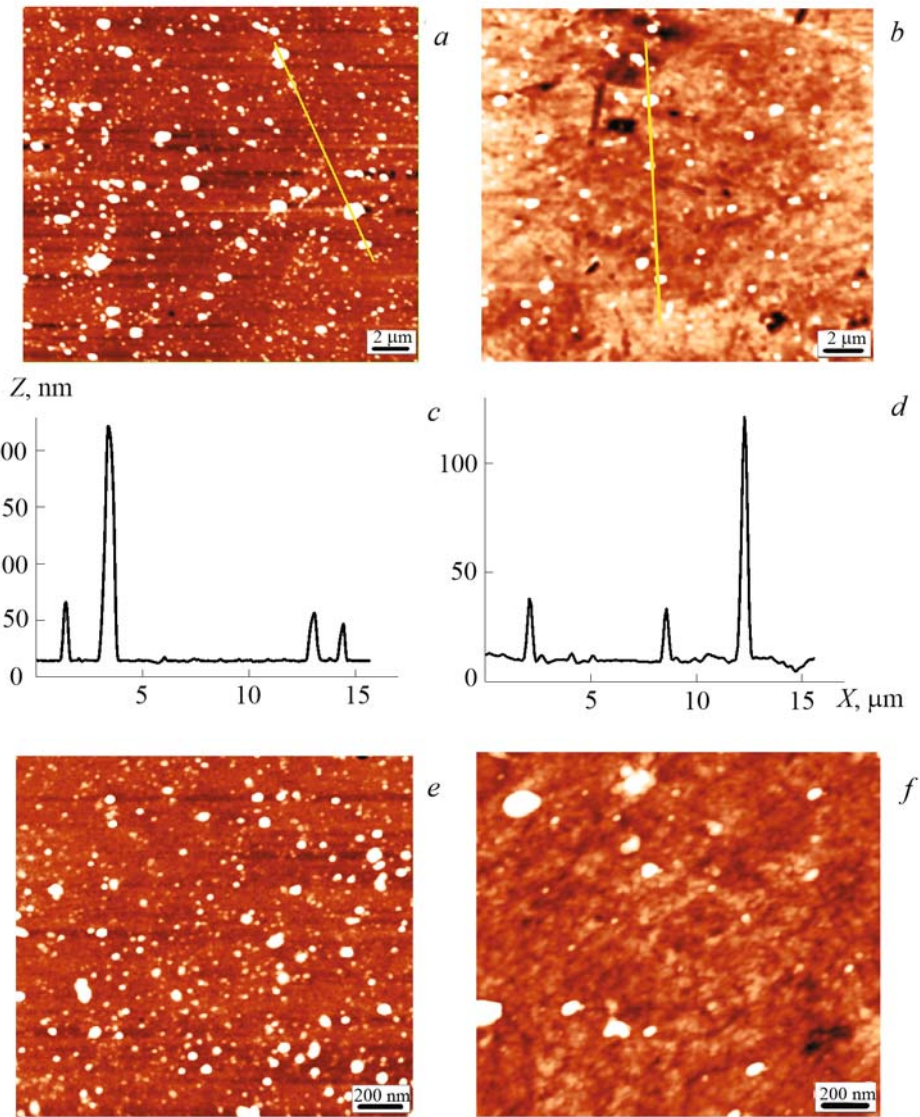


Fig. 1. AFM images of the surface morphology (a, b, e, f) and the cross section profile along selected line (c, d) of laser-deposited thin zirconium film on silicon (a, c, e) and glass substrates (b, d, f).

In the present work the structural, optical, and electric characteristics of thin films of zirconium vacuum deposited on silicon and glass substrates by multipulse high frequency laser action [11] were investigated.

Experimental Setup and Methods of Investigation. The Zr films were deposited by high-frequency laser sputtering on ceramic targets under vacuum ($p = 2.2 \text{ Pa}$). The experimental setup ($\lambda = 1.06 \mu\text{m}$) with an adjustable pulse repetition rate of 5–50 kHz consisted of a laser radiation source, an optical system for transferring the laser radiation to the target, a vacuum chamber, and a measurement and diagnostic module. The pulse repetition rate was varied by changing the laser pump level and the optical density of the shutter made of irradiated crystalline lithium fluoride (LiF) with F_2^- color centers and a laser pulse length $\tau \sim 85 \text{ ns}$. The deposition of macroscopically homogeneous thin films was achieved with laser radiation power density $q = 120 \text{ MW/cm}^2$ and pulse repetition frequency $f \sim 6\text{--}10 \text{ kHz}$.

Atomic-force microscopy (AFM) was used to investigate the surface morphology and to determine the principal roughness parameters of the Zr films. The measurements were made on a Solver P47 Pro scanning probe microscope (NT-MDT, Russia); standard cantilevers for contactless methods with resonance frequency $\omega = 230 \text{ kHz}$ and stiffness coefficient 15.1 N/m were used as probe sensors. The radius of curvature of the needle tip was $< 3 \text{ nm}$. The transmission

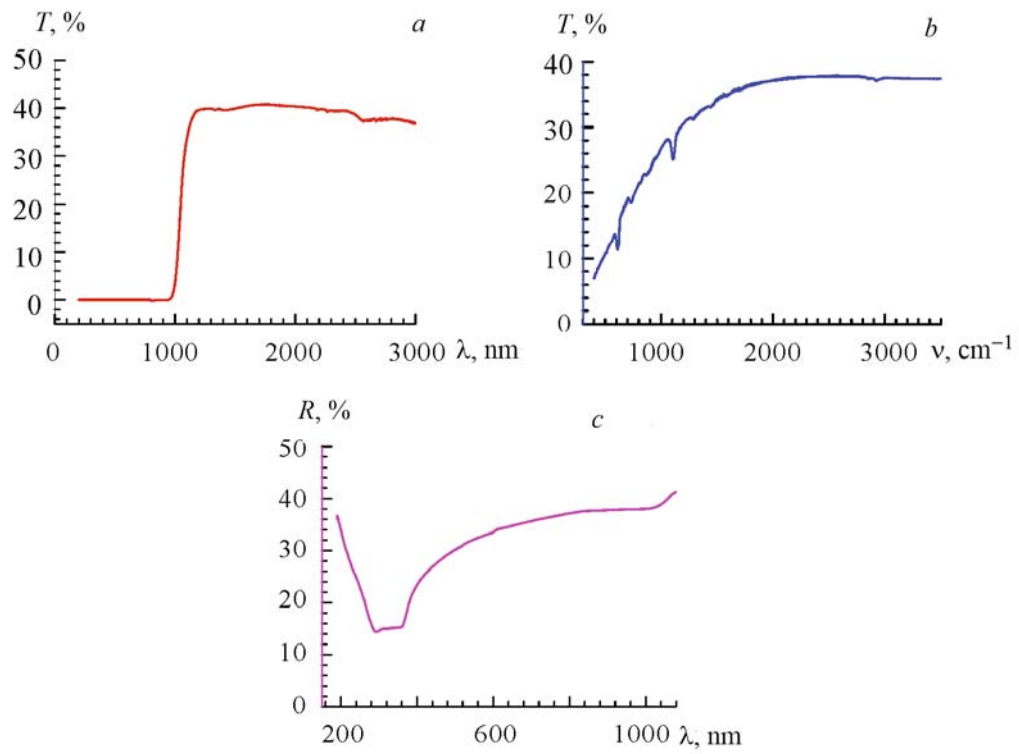


Fig. 2. The transmission spectrum of the laser-deposited film of zirconium on a silicon substrate in the visible and near-IR regions (a) and the mid-IR region (b); the reflection spectrum of the laser-deposited film of zirconium on a silicon substrate in the visible and near-IR regions (c).

of the optical radiation by the thin films in the near-IR region was measured on a Carry 500 Scan spectrophotometer. The transmission spectra in the mid-IR region were recorded on a NEXUS IR-Fourier spectrometer (Thermo Nicolet) in the region of 400–4000 cm⁻¹. Measurements of the current–voltage characteristics (CUV) and capacitance–voltage (CAV) characteristics were made on an E7-20 immittance meter at room temperature with signal frequencies of 100 kHz and 1 MHz.

Results and Discussion. By the AFM method in the amplitude-modulation frequency mode it was established that high-frequency laser sputtering of the target under vacuum leads to the deposition of a nanocrystalline thin film of Zr on the silicon and glass substrates (Fig. 1). The main roughness parameters of the surface morphology were determined at five different points on the sample with scanning of an area of 20 × 20 μm. The average size of the structural elements of the Zr film on the silicon substrate was 15 nm with a mean-square roughness of 6.2 nm. A small number of large formations with height of up to 250 nm and lateral size of 0.5–1.2 μm were observed on the surface of the films (Fig. 1c). The average height of the surface relief of the films on the glass substrate was ≤11 nm, and the root-mean-square roughness was 3.4 nm. Significantly fewer large formations were observed on the glass substrate than on the silicon substrate, and their height was in the region of 40–120 nm with a lateral dimension of 0.3–0.6 nm (Fig. 1d).

A sharp jump in the transmission of the laser-deposited Zr film on silicon is observed in the near-IR region $\lambda = 953\text{--}1190$ nm in the region of $T = 0.1\text{--}39.5\%$. The transmission in the region of 1190–2890 nm is $T \sim 40\%$ (Fig. 2a). The transmission of the film in the mid-IR region remains constant at $T \sim 37\%$ in the frequency range of $\nu = 1960\text{--}3490$ cm⁻¹ (Fig. 2b). The coefficient of reflection R (Fig. 2c) decreases in the region of $\lambda = 190\text{--}280$ nm, remains constant at $\lambda = 286\text{--}360$ nm, and increases smoothly to $\lambda = 1020$ nm.

The current–voltage CUV and capacitance–voltage CAV characteristics of the Zr film on the Si substrate are shown in Fig. 3. As seen, the CUV curve is practically symmetrical. At positive voltages the dependence of the current on the voltage is close to linear. In the region of negative voltages a small amount of hysteresis is observed on the CUV. This may be due to the complex relationship for the film formed during deposition at the interface, including deposition with the oxide and the presence of a high series resistance. The Zr/Si structure has a frequency- and voltage-dependent CAV

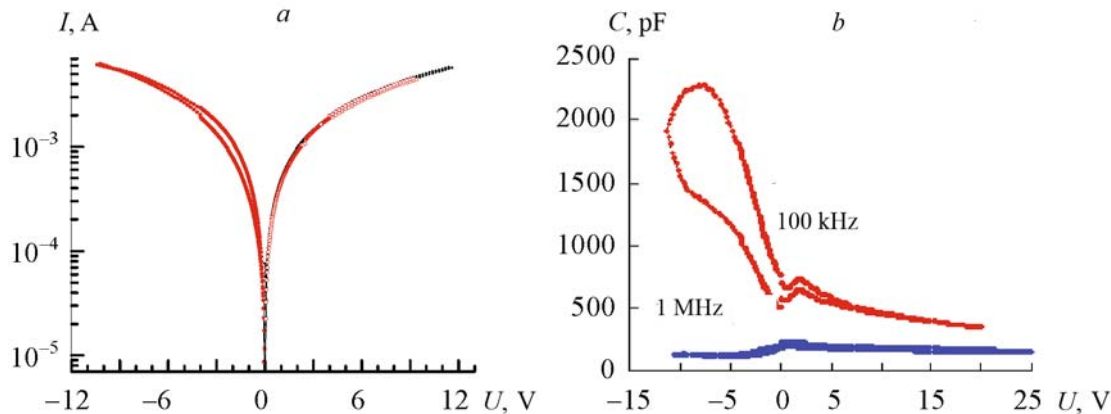


Fig. 3. Voltage–current (a) and voltage–capacitance (b) characteristics of the thin film of zirconium on silicon.

(Fig. 3b). The dependence of the capacitance on the voltage arises from the characteristic behavior of the depleted layer formed on the surface of the semiconductor and also on the presence of series resistance and interface states. The frequency dependence is due to the presence of series resistance and localized interface states at the interface. At low frequencies (100 kHz) the measured capacitance is equal to the equivalent of the capacitance of the interface states, the capacitance of the interfacial layer, and the space charge capacitance. As the frequency of the applied alternating signal increases the interface states are no longer completely filled, and the contribution from the interface states to the contact capacitance decreases. The capacitance of the structure therefore decreases with increase of the frequency. For the CAV of the investigated sample with the application of a positive voltage of ~ 1 V a maximum is observed at the high frequency of 1 MHz, which may be due to a stronger change in the capacitance of the barrier layer and to the frequency characteristics of the surface states of the interface. On account of the strong contribution from the Zr/Si interface (the presence of the rapid surface states) the switching processes are quite difficult to observe in samples with high conductivity. The presence of hysteresis on the CAV indicates a built-in charge, and $|\Delta U| = 2.4$ V at 100 kHz while at 1 MHz $|\Delta U| = 1.4$ V. This may be due to the presence of the built-in charge of the thin layer of oxide at the interface.

Conclusions. Thin films of zirconium with a fairly uniform surface structure were produced. The average height of the surface of the films on silicon was not greater than 15 nm with mean-square roughness of 6.2 nm. An insignificant amount of large formations with height above 250 nm was observed. The average height of the film microprotrusions on the glass substrate was not greater than 11 nm, and the root-mean-square roughness was 3.4 nm, while a small number of large formations of up to 120 nm in height were observed. On the film on the silicon substrate a reflection minimum was observed in the region of $\lambda = 286\text{--}360$ nm. On account of the high series resistance the Zr/Si structure shows nonideal current-voltage characteristics. The presence of high series resistance and built-in charge at the Zr/Si interface restricts the forward current and does not lead to a rectification effect, which is explained by an imperfect ohmic contact. Further research to improve the ohmic contact is needed in order to produce Zr/Si metal–semiconductor Schottky diodes with low saturation current. The obtained thin zirconium films on a silicon substrate can be used in multilayer optical coatings with high thermal and chemical resistance and for clarification in the visible and near-IR spectral regions.

REFERENCES

1. L. M. Lynkov, T. V. Molodechkina, V. A. Bogush, and T. V. Borbotko, *Dokl. BGUIR*, No. 3, 73–84 (2004).
2. Xu Jinping, Bai Tiecheng, Li Xingjiao, Zheng Xiangbin, Su Wuda, and An Changwu, *Vacuum*, **43**, No. 11, 1051–1053 (1992).
3. N. E. Nekrasova and S. S. Kruglikov, *Fizikokhim. Poverkh. Zashch. Mater.*, **47**, No. 6, 668–672 (2011).
4. S. V. Ivanova, É. M. Glagovskii, V. K. Orlov, I. A. Shlepov, K. Yu. Nikonorov, V. V. Rozhko, V. A. Glebov, and S. Ya. Betzofen, *Yadern. Fiz. Inzhiniring*, **2**, No. 3, 224–234 (2011).
5. D. G. Olmedo, D. R. Tasat, P. Evelson, R. Rebagliatti, M. B. Guglielmotti, and R. L. Cabrini, *J. Biomed. Mater. Res. A*, **98A**, No. 4, 604–613 (2011).

6. R. H. Nielsen, J. H. Schlewitz, and H. Neilson, *Kirk-Othmer Encycl. Chem. Technol.* (2000), pp. 1–46.
7. S. Q. Hussain, S. Kim, S. Ahn, N. Balaji, Y. Lee, J. H. Lee, and J. Yi, *Solar Energy Mater. Solar Cells*, **122**, 130–135 (2014).
8. B. Zhang, X. Dong, X. Xu, P. Zhao, and J. Wu, *Solar Energy Mater. Solar Cells*, **92**, No. 10, 1224–1229 (2008).
9. D. A. Aldemir, *Modern Phys. Lett. B*, **34**, No. 10, Article ID 2050095 (2020).
10. E. H. Rhoderick, *IEE Proc. I, Solid-State Electron. Dev.*, **129**, No. 1, 1–4 (1982).
11. L. Ya. Minko, A. N. Chumakov, and N. A. Bosak, *Kvantovaya Elektron.*, **17**, No. 11, 1480–1484 (1990).